

SURFACE IMPEDANCE OF HIGH T_c SUPERCONDUCTORS

L. Drabeck, J. Carini, and G. Grüner
 Department of Physics and Solid State Science Center
 University of California, Los Angeles 90024

and
 T.L. Hylton, A. Kapitulnik, and M.R. Beasley
 Department of Physics, Stanford University, Stanford, California 94305

ABSTRACT

The surface impedance of various high temperature superconductors has been examined in the millimeter wave spectral range. The ceramic, thin film and single crystal samples are characterized by a residual surface resistance $R_s(T \rightarrow 0)$ and a temperature dependent contribution $R_s(T)$. $R_s(T \rightarrow 0)$ is accounted for by a model of Josephson coupled grains. The surface resistance exceeds the Mattis-Bardeen limit in both ceramic and thin film specimens.

The surface impedance of the recently discovered high temperature superconductors is an important parameter for determining the application potential of these materials. The surface resistance R_s has been investigated by several groups^{1,2,3}, mainly in ceramic materials and at microwave frequencies. We report extensive measurements in both ceramics⁴ and thin films^{5,6} in the millimeter wave spectral range.

For a superconductor, with a complex conductivity $\sigma = \sigma_1 - j\sigma_2$, the surface impedance

$$Z_s = \left(\frac{j\mu_0\omega}{\sigma_1 - j\sigma_2} \right)^{1/2} = R_s + jX_s \quad (1)$$

can be calculated assuming certain temperature dependence for σ_1 and σ_2 which relies on the detailed form of the superconducting state properties, such as gap anisotropy, mean free path, etc. Both σ_1 and σ_2 can be evaluated⁷ using weak coupling BCS theory for an isotropic gap Δ at various temperatures. The overall temperature (T) and frequency (ω) dependence at low temperature (i.e. $k_B T \ll \Delta$) is

$$R_s = A \frac{\Delta}{T} \left(\frac{\omega^2}{\Delta^2} \right) \ln \left(\frac{\Delta}{\hbar\omega} \right) \exp \left(- \frac{\Delta}{k_B T} \right), \quad (2)$$

where A is a numerical factor reflecting the properties of the normal state at $T > T_c$. The exponential behavior is a consequence of the gap, while the ω^2 dependence of R_s reflects the inductive response of the superfluid. In contrast, for a normal metal R_s and X_s are proportional to $\omega^{1/2}$.

We have measured R_s and X_s by employing resonant cavities which operate at 100 GHz and 150 GHz⁸. The superconducting material or a polished copper plate forms the bottom part of the TE011 resonance cavity and the resonance frequency and bandwidth are measured as a function of temperature. The difference between the sample surface impedance and the copper surface impedance is proportional to the change in bandwidth $\Delta W = W_{\text{sample}} - W_{\text{Cu}}$ and the resonance frequency $\Delta f = f_{\text{sample}} - f_{\text{Cu}}$:

$$\Delta Z_s = \Delta R_s + j\Delta X_s = \gamma^{-1} (\Delta W/2 - j\Delta f), \quad (3)$$

where γ is the resonator constant for the mode.

Ceramic materials were made by the well known technique⁴. The $\text{YBa}_2\text{Cu}_3\text{O}_{7-\delta}$ thin films were prepared by reactive magnetron co-sputtering from three metal targets in an oxygen background onto (100) SrTiO_3 substrates. The $\text{Y}_2\text{Ba}_4\text{Cu}_8\text{O}_{16-\delta}$ films were electron beam evaporated rather than sputtered, and BaF_2 was used instead of a metallic Ba target. The films are disordered as deposited. Epitaxial films result after high temperature oxygen annealing. The compositions of the films were very close to the 1:2:3 and 2:4:8 stoichiometry, with a compositional variation across the film of about 1 at. %. The films were polycrystalline. $\text{Bi}_2\text{CaSr}_2\text{Cu}_2\text{O}_8$ single crystals were grown by the standard techniques for these materials.

The temperature dependence of R_s is

displayed in Fig. 1, with the full line being the calculated R_s based on the Bardeen-Cooper-Schrieffer (BCS) theory⁷. The ceramic materials were found to have large residual losses $R_s(T \rightarrow 0)$, typically 0.65Ω at 100 GHz⁴ and losses are also high for the Bi single crystal. The thin films represent a significant improvement, with oriented films at 150 GHz giving $R_s(T \rightarrow 0) = 0.070 \Omega$ for the 123 film and $R_s(T \rightarrow 0) = 0.020 \Omega$ for the 248 film⁵. It is also evident from the figure, that the losses are two orders of magnitude larger than that predicted by the BCS theory even if $R_s(T)$ is regarded as the surface resistance reflecting the contributions of carriers excited across the single particle gap. Also, at low temperatures, c-axis films consistently show $R_s(T) - R_s(T=0) \sim T^{5,6}$ in contrast to the exponential behavior predicted by BCS theory. Our measurements of the c-axis oriented films are consistent with an ω^2 frequency dependence of the surface resistance in the millimeter wave spectral range⁶.

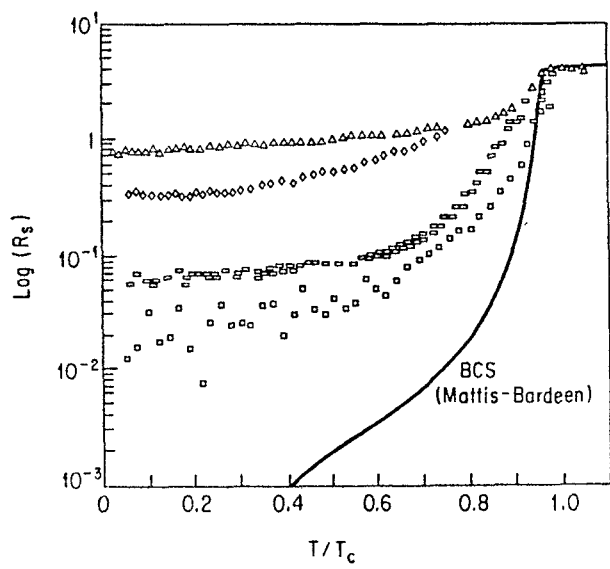


Fig. 1. Temperature dependence of the surface resistance in ceramic $\text{YBa}_2\text{Cu}_3\text{O}_7$ (Δ), thin film 123 (rectangle), thin film $\text{Y}_2\text{Ba}_4\text{Cu}_8\text{O}_{16}$ (square), and in a $\text{Bi}_2\text{CaSr}_2\text{Cu}_2\text{O}_8$ single crystal (diamond) at 150 GHz. The full line is calculated from the BCS model assuming weak coupling and an isotropic gap.

We have also measured the penetration depth λ_{eff} by measuring the dc or low frequency susceptibility of specimens with dimensions comparable to λ_{eff} , or by examining the surface reactance X_s . The latter is, at low temperature, proportional to λ_{eff} . The London penetration depth, $\lambda_L = (c/\omega_p)$ where c is the speed of light and $\omega_p = 2.5$ eV is the plasma frequency, is calculated to be $\lambda_L = 1500 \text{ \AA}$. λ_{eff} is expected to exceed this value due to increased penetration caused by irregularities such as grain boundaries, second phases, etc. We have indeed found that $\lambda_{\text{eff}} > \lambda_L$ and the values obtained are displayed in Fig. 3. The temperature dependence of λ_{eff} measured by magnetization in the case of ceramics and by measuring the surface reactance X_s in thin films is displayed in Fig. 2. The full line is $\lambda_L(T)$ calculated on the basis of the BCS model.

The residual losses are most likely the result of inhomogeneities, second phases, grain boundaries, etc. We have developed a simple model to describe the effect of grain boundaries on the surface impedance^{9,10}. The film is modeled as a network of superconducting grains of dimension 'a' coupled by Josephson junctions, which we describe as the standard resistively shunted junction with negligible capacitance. The kinetic inductivity of the grains is $L_G = \mu_0 \lambda^2$ where λ is the penetration depth of the grains, while the unit areal inductance of the junction is $L_j = \hbar/2eJ_c$ with J_c the critical current of the junction. The shunt resistance of the junction is R . In the limit, where the conductance is dominated by the inductive channel, the surface impedance is given by

$$Z_s = R_s + j X_s \quad (4)$$

$$X_s = \omega \mu_0 \left(\lambda_L^2 + \lambda_j^2 \right)^{1/2} \quad (4a)$$

$$R_s = \frac{1}{2} \omega \mu_0 \frac{\lambda_j^2}{(\lambda_L^2 + \lambda_j^2)} \frac{\hbar \omega}{2eI_c R} \quad (4b)$$

where λ_j is the effective continuum penetration depth due to the network of grain boundaries alone, and is significantly larger than the London penetration depth λ_L . In the limit of a uniform film with vanishing Josephson effect, the penetration depth

$$\lambda_{\text{eff}} = (\lambda_L^2 + \lambda_j^2)^{1/2} \quad (5)$$

equals the London penetration depth λ_L , and $R_s = 0$. With increasing λ_j , due to the increased number of boundaries, both λ_{eff} and R_s are determined by λ_L , λ_j , and the $I_c R$ product. The model leads to R_s which is proportional to ω^2 , and this has been established by several recent experiments on $\text{YBa}_2\text{Cu}_3\text{O}_7$.

In addition to establishing R_s ($T \rightarrow 0$) and λ_{eff} ($T \rightarrow 0$) we have also found^{5,6} that in all of our specimens the temperature dependence of the penetration depth is given, at $T \ll T_c$ by

$$\lambda(T) - \lambda(0) = AT^2 \quad (6)$$

In Fig. 3 we display λ_{eff} and A as a function of R_s ($T \rightarrow 0$), where we have also included both λ_{eff} and R_s measurements^{3,12} on single crystals. We recover the expected correlation between R_s and λ_{eff} , namely, with increased sample quality (i.e. $R_s \rightarrow 0$), λ_{eff} approaches the London penetration depth $\lambda_L = 1500 \text{ \AA}$. In our proposed model, this would correspond to a larger grain size and thus a smaller number of junctions in the film. In addition, the coefficient A which characterizes the temperature dependent part of λ , also approaches zero, indicating that within experimental error $\lambda(T) - \lambda(0)$ agrees with the negligible temperature dependence at low temperatures as given by the BCS ground state.

In conclusion, our experiments on $\text{YBa}_2\text{Cu}_3\text{O}_7$ ceramics and thin films and on (evidently fairly poor quality) $\text{Bi}_2\text{CaSr}_2\text{Cu}_2\text{O}_8$ single crystals give effective penetration lengths which exceed the London penetration depth and finite and significant surface impedance in the micro and millimeter wave spectral range. We find both R_s and λ_{eff} decrease with increasing sample quality, and the temperature dependence of λ approaches the form expected for singlet pairing. These observations are in agreement with a model where the surface impedance is dominated by losses and effective magnetic field penetration caused by Josephson type effects at grain boundaries.

Work at University of California (Los Angeles, CA) was supported by the Office of Naval Research. Work at Stanford was supported by the National Science Foundation. One of us (T.H.) would like to thank AT&T for partial support.

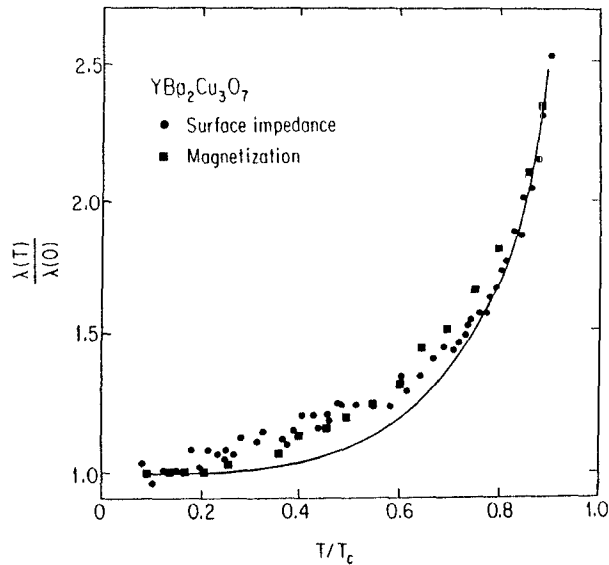


Fig. 2. Temperature dependence of the effective penetration depth as measured by magnetization¹¹ or surface reactance⁵. The full line is calculated from the BCS model.

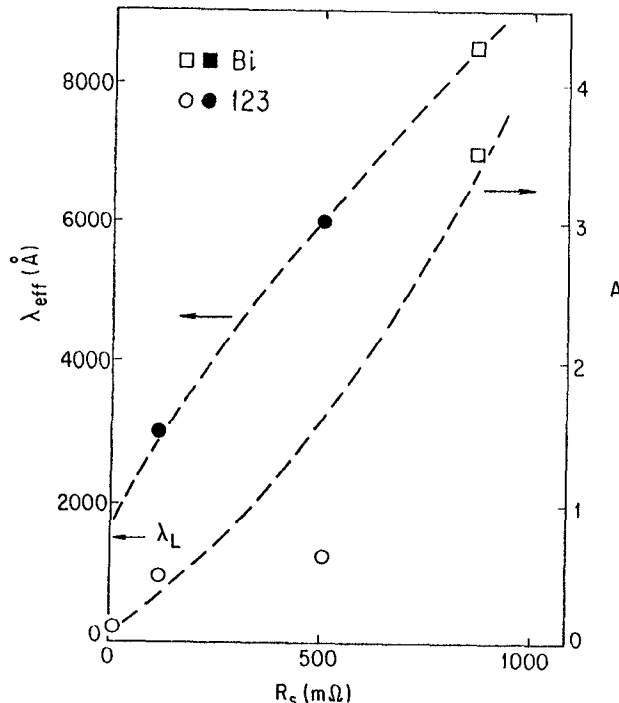


Fig. 3. Effective penetration depth λ_{eff} and the coefficient A of Eq. (6) versus the zero temperature surface resistance R_s ($T \rightarrow 0$). For the various values and error bars, see the references quoted in the text.

REFERENCES

1. For a short review see J. Carini, L. Drabeck, and G. Grüner, *Modern Phys. Lett.* B3, 5 (1989).
2. S. Sridhar, C. Shiffman, and H. Hamdeh, *Phys. Rev.* B36, 2301 (1988). A. Fathy, D. Kalokitis, and E. Belohouber, *Microwave Journal* Oct. 1988.
3. D.L. Rubin, et. al., *Phys. Rev.* B38, 6538 (1988).
4. A. Awasthi, J. Carini, B. Alavi, G. Grüner, *Solid State Comm.* 67, 373 (1988).
5. L. Drabeck, J. Carini, G. Grüner, T. Hylton, K. Char, M. Beasley, *Phys. Rev.* B39, 785 (1989).
6. J. Carini, A. Awasthi, W. Beyermann, G. Grüner, T. Hylton, K. Char, M. Beasley, A. Kapitulnik, *Phys. Rev.* B37, 9726 (1988).
7. D.C. Mattis and J. Bardeen, *Phys. Rev.* 111, 412 (1958).
8. L. Drabeck, W. Beyermann, J. Carini, G. Grüner, unpublished.
9. T. Hylton, A. Kapitulnik, M. Beasley, J. Carini, L. Drabeck, G. Grüner, *Appl. Phys. Lett.* 53, 1343 (1988).
10. T. Hylton and M. R. Beasley (to be published).
11. J. Cooper, et. al., *Phys. Rev.* B37, 638 (1988).
12. L. Krusin-Elbaum, et. al., *Phys. Rev. Lett.* 62, 217 (1989). D. R. Harshman, et. al., *Phys. Rev.* B39, 851 (1989).